



UNIVERSITY OF LEEDS

This is a repository copy of *Erratum: 'Mechanically robust waveguide-integration and beam shaping of terahertz quantum cascade lasers'*.

White Rose Research Online URL for this paper:
<http://eprints.whiterose.ac.uk/87467/>

Version: Accepted Version

Article:

Valavanis, A, Han, YJ, Brewster, N et al. (9 more authors) (2015) Erratum: 'Mechanically robust waveguide-integration and beam shaping of terahertz quantum cascade lasers'. *Electronics Letters*, 51 (13). 1037 - 1037 (1). ISSN 1350-911X

<https://doi.org/10.1049/el.2015.1930>

Reuse

Unless indicated otherwise, fulltext items are protected by copyright with all rights reserved. The copyright exception in section 29 of the Copyright, Designs and Patents Act 1988 allows the making of a single copy solely for the purpose of non-commercial research or private study within the limits of fair dealing. The publisher or other rights-holder may allow further reproduction and re-use of this version - refer to the White Rose Research Online record for this item. Where records identify the publisher as the copyright holder, users can verify any specific terms of use on the publisher's website.

Takedown

If you consider content in White Rose Research Online to be in breach of UK law, please notify us by emailing eprints@whiterose.ac.uk including the URL of the record and the reason for the withdrawal request.



eprints@whiterose.ac.uk
<https://eprints.whiterose.ac.uk/>

Mechanically robust waveguide integration and beam shaping of terahertz quantum cascade lasers

A. Valavanis, Y. J. Han, N. Brewster, P. Dean, R. Dong, L. Bushnell, M. Oldfield, J. X. Zhu, L. H. Li, A. G. Davies, B. Ellison and E. H. Linfield

Terahertz-frequency quantum cascade lasers (THz QCLs) have numerous potential applications as 1–5 THz radiation sources within space-science, biomedical and industrial sensing scenarios. However, key obstacles to their widescale adoption outside laboratory environments have included their poor far-field beam quality and the lack of mechanically robust schemes that allow integration of QCLs with THz waveguides, mixers and other system components. In this letter, we present a block integration scheme in which a continuous-wave ~ 3.4 THz double-metal QCL is bonded into a precision-machined rectangular waveguide within a copper heat-sink block. This highly-reproducible approach provides a single-lobed far-field beam profile with a divergence $\lesssim 20^\circ$, and with no significant degradation in threshold current or range of operating temperature.

Introduction: Terahertz-frequency quantum cascade lasers (THz QCLs) [1] are compact sources of coherent radiation in the 1–5 THz band, with peak output powers up to 1 W [2]. Numerous potential applications exist, including their use as local-oscillators for satellite-borne astronomy and atmospheric science instrumentation [3] and as radiation sources for industrial inspection, security and biomedical imaging [4]. However, widespread commercialisation of THz QCLs has not yet been realised. One significant issue is the lack of a mechanically robust and reproducible scheme for integrating THz QCLs with external waveguides and mixers. This typically leads to large and fragile arrangements of discrete optical components, although several elegant yet complex semiconductor integration techniques have been proposed (e.g. [5]). QCLs in double-metal waveguides yield the best thermal performance, and are well-suited to *near-field* radiation coupling (e.g., into external waveguides). However, their poor *far-field* beam quality and wide divergence [6] leads to poor coupling into external free-space optical components. Previous beam optimisation techniques have employed either device patterning approaches [7, 8] or assemblies of antennas or lenses [9, 10]. Although far-field beam divergence of $\lesssim 20^\circ$ is achievable with these techniques, they are relatively complex and their reproducibility and mechanical robustness have not been demonstrated.

We report a new packaging and waveguide-integration scheme, in which a 3.4-THz double-metal QCL is ribbon-bonded to a dc stripline within a copper heat-sink enclosure containing a rectangular cross-section metallic waveguide. This approach makes use of highly-reproducible mechanical microfabrication techniques previously developed to support construction of waveguide-integrated THz-frequency mixers. Since the QCL cavity itself is not modified, this approach has very low impact on the threshold current and operating temperature range of the device, while yielding a beam divergence of $< 20^\circ$, comparable to the previous techniques discussed above.

QCL fabrication: The QCL used in this work was based on a 3.5-THz bound-to-continuum active region design [11]. The device was grown using molecular-beam epitaxy on a semi-insulating GaAs substrate. A 300-nm-thick $\text{Al}_{0.5}\text{Ga}_{0.5}\text{As}$ etch-stop layer was followed by a 100-nm-thick Si-doped n^+ -GaAs contact layer ($N = 5 \times 10^{18} \text{ cm}^{-3}$). 120 periods of the active-region structure were grown on top of this, to a total thickness of 14 μm , followed by a 50-nm-thick n^+ -GaAs contact layer. 10/500 nm Ti/Au was deposited on top of the wafer, and a second n^+ -GaAs acceptor wafer. The two wafers were thermal-compression bonded at the metallic interfaces and devices were processed into Au–Au waveguide structures using wet chemical etching [12]. Lasers were processed in arrays of 13 parallel ridges with 110- μm width using a Ti/Au (10/150 nm) film as the top waveguide. The distance between the processed ridges was 100 μm . The substrate was thinned and metallised to improve thermal performance, and the ridges were cleaved to a length of 980 μm .

One set of ridges was bonded into the new waveguide/heat-sink block as described in the next section, while another was indium soldered onto

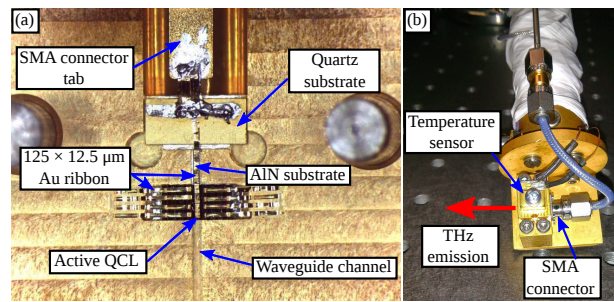


Fig. 1 (a) Interior of the bottom half of the waveguide block, showing the integrated QCL, waveguide channel and electrical contact components. (b) Exterior of QCL waveguide block, mounted on cold-finger of a helium cryostat, showing the integrated SMA connector and temperature sensor.

a conventional copper planar submount to provide a comparison between our new packaging scheme and conventional ‘unmounted’ devices. In the latter case, electrical biasing terminals were made using Au wire bonds to Au-coated ceramic pads on the Cu submount.

Waveguide block: A channel of cross-sectional dimensions $300 \times 75 \mu\text{m}^2$ was precision-machined directly into a copper block, which also contained a cavity for locating the QCL device. A second identical channel was machined into another copper block and the two halves co-registered to form a full-height rectangular waveguide structure of aperture $300 \times 150 \mu\text{m}^2$. The QCL array was placed in the cavity in the lower block, as shown in Fig. 1(a), upon a 20- μm -thick layer of In foil to ensure a good thermal contact. This method allowed readjustment of the QCL position and allows easy replacement of devices within the block. The output facet of the central QCL ridge in the array was aligned with the waveguide aperture (with the other devices being left unused), and a $125 \times 12.5 \mu\text{m}^2$ Au ribbon bond wire was used to provide an electrical direct current (dc) or pulsed bias connection to the top contact of the QCL.

Additional Au ribbon bonds between the top surfaces of the unused devices and the copper block provided mechanical compression when the two halves of the block were combined, thus establishing a good thermal interface between the QCL and the copper surface. As an additional measure to ensure adequate heat sinking of the bias connection, and also to ease device assembly, a small gold-plated strip of AlN and a gold-plated quartz substrate were incorporated and provided intermediate bonding pads between the QCL and the dc bias connector. The pads were secured to the copper block by high conductivity silver loaded epoxy.

The complete assembled block is shown in Fig. 1(b), mounted onto the cold-finger of a Janis ST-100 liquid-helium cryostat. The electrical bias is supplied through a subminiature (SMA) connector on the rear of the block (i.e., the opposite side from the emission aperture), and the temperature is monitored at the top of the block using a LakeShore DT-470 silicon diode.

Power and spectral mapping: For pulsed characterisation, the QCL was driven using a 10-kHz, 2% duty-cycle current pulse train, which was modulated using a 167-Hz square-wave to match the peak responsivity of a helium-cooled Ge:Ga bolometric detector. The threshold current was measured as $I_{\text{th}} = 130 \text{ mA}$ at a heat-sink temperature of 10 K, using an inductive current probe. THz emission was observed up to a maximum operating heat-sink temperature, T_{max} , of 90 K. This compares favourably with the performance of an equivalent, ‘unmounted’ device (c.f., $I_{\text{th}} = 100 \text{ mA}$, $T_{\text{max}} = 97 \text{ K}$).

For continuous wave (cw) operation, the QCL was driven using a dc power supply, and the beam was modulated at 185 Hz using an optical chopper. The block-integrated device was again found to have a low-temperature (20 K) threshold current, $I_{\text{th}} = 130 \text{ mA}$ while the maximum operating temperature reduced to $T_{\text{max}} = 77 \text{ K}$. Again, this compares favourably with the unmounted device ($I_{\text{th}} = 100 \text{ mA}$, $T_{\text{max}} = 80 \text{ K}$).

These results imply that the mounting scheme introduces no significant thermal or electronic perturbation to the laser performance. Indeed, any increase in the internal thermal resistance or power dissipation in the device would have been manifested as an increase in the cw threshold current. Furthermore, the small T_{max} offset between the two devices was found to be almost independent of the duty-cycle of the driving current. The temperature offset between the sensors on the QCL

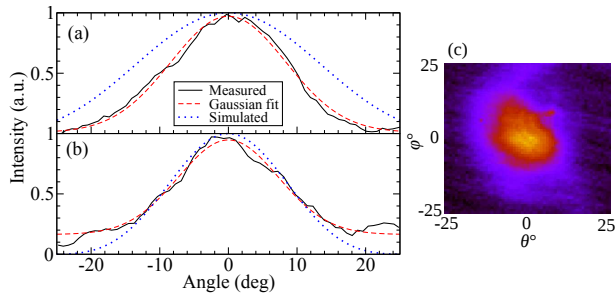


Fig. 2 Cross-sections of the far-field beam profile (a) along the axis of epitaxial growth, θ and (b) in-plane with the device substrate, ϕ , and (c) a two-dimensional image of the beam profile.

block and the cryostat cold-finger was also found to be negligible ($\lesssim 2$ K) under all driving conditions.

The emission spectra of the two devices were measured using an FTIR spectrometer. In each case, a similar spectral bandwidth (~ 120 GHz) and centre frequency (~ 3.38 THz) were observed, supporting our conclusion that the mounting scheme does not introduce any significant perturbation to the internal properties of the laser.

The peak THz power emitted from the device was estimated at 20 K, using an absolute THz power meter, to be $340 \mu\text{W}$ in pulsed mode, and $30 \mu\text{W}$ in cw operation. In both cases, this is approximately 20% of the value measured for the equivalent unmouted device (1.5 mW and $120 \mu\text{W}$ respectively). Nevertheless, the absolute THz power emission is already sufficient for the development of applications.

Although there is a notable reduction in the absolute THz power, this is not accompanied by any other significant change in device performance. We therefore attribute this to a mismatch between the transverse mode profile of the laser cavity and that of the relatively-wide rectangular waveguide, and between the waveguide aperture and free space. However, this is not a fundamental issue, and it is important to note that as a first exploratory development step, the waveguide cross-section dimensions were selected on the basis of easing mechanical construction and simplifying the QCL-waveguide interface. At 3.4 THz, however, the waveguide can in principle sustain multiple field modes, which is undesirable as it may affect output beam quality and coupling to external devices, e.g. a detector diode. A future development will use a reduced waveguide aperture size to ensure that the electrical field is constrained to a fundamental mode of operation.

Beam profiles: The far-field beam profile of the block-integrated QCL was measured using a Golay detector with an entrance aperture of 1-mm diameter, positioned at a longitudinal distance of 32.4 mm from the laser facet. This is significantly larger than the Fraunhofer distance (5.8 mm) for the emitter, ensuring that a true far-field pattern was observed. The laser was driven using a continuous 30-Hz square wave, and operated at a heat-sink temperature of 30 K. The detector was scanned linearly in two dimensions over a 30×30 -mm² area, using a 0.5-mm step size in each direction. The beam intensity, sampled at each position, was transformed into rotational coordinates along the epitaxial growth axis (θ), and in parallel with the substrate (ϕ).

Fig. 2 shows that an approximately Gaussian single-lobed profile can be fitted to the far-field in both directions, and that the ‘ringing’ that is commonly associated with the beam profiles of unmouted double-metal QCLs has been removed entirely. The full-width at half-maximum (FWHM) in the growth and in-plane directions is 20° and 17° respectively. This is comparable to the divergence obtained previously by patterning the QCL or through the use of device-integrated antenna structures or lenses [7, 8, 9, 10].

The field pattern of the open-ended waveguide was calculated by transforming the aperture field to the far-field using bespoke electromagnetic modelling code. Fig. 2 shows that the simulated FWHM of 30° and 20° for the growth and in-plane directions are in reasonable agreement with the measured values. The discrepancy in the simulated pattern (for the growth direction) may be attributed partly to the assumptions within the model that the waveguide is single-moded, and that fringe effects from the waveguide walls are negligible.

Conclusion: We have demonstrated a new waveguide integration scheme for THz QCLs, which is based on a highly-reproducible precision-micromachining technique. This approach yields a beam divergence of $< 20^\circ$ and eliminates the spatial ‘ringing’ commonly seen in double-metal QCL beam profiles, without the need for any complex device-specific semiconductor processing techniques. The block integration has been shown not to introduce any significant degradation in the threshold current or operating temperature range.

The complete enclosure of the QCL within a metallic block potentially adds a degree of protection against mechanical impacts, and shielding against exposure to ionising radiation, both of which are essential for the deployment of THz QCLs in satellite-based applications. Future development activity will pursue the integration of a Schottky diode within the waveguide structure to form a complete THz heterodyne mixer.

Acknowledgment: We acknowledge financial support from the EPSRC (UK) ‘COTS’ programme, the ERC grants ‘NOTES’ and ‘TOSCA’, NERC (UK), CEOI (UK) and the European Space Agency. A.G.D. acknowledges support from the Royal Society and the Wolfson Foundation. P.D. acknowledges support from EPSRC (UK).

This is an open access article published by the IET under the Creative Commons Attribution License (<http://creativecommons.org/licenses/by/3.0>)

April 2, 2015

doi: 10.1049/el.2015.xxxx

A. Valavanis, Y. J. Han, P. Dean, R. Dong, J. X. Zhu, L. H. Li, A. G. Davies, and E. H. Linfield (*School of Electronic and Electrical Engineering, University of Leeds, Leeds, LS2 9JT, UK*)

N. Brewster, L. Bushnell, M. Oldfield, and B. Ellison (*Rutherford Appleton Laboratory, STFC, Harwell Oxford, Didcot, OX11 0QX, UK*)

E-mail: a.valavanis@leeds.ac.uk

References

- Köhler, R., Tredicucci, A., Beltram, F., Beere, H.E., Linfield, E.H., Davies, A.G., Ritchie, D.A., Iotti, R.C., and Rossi, F., ‘Terahertz semiconductor-heterostructure laser’, *Nature*, 2002, **417**, pp. 156–159
- Li, L., Chen, L., Zhu, J., Freeman, J., Dean, P., Valavanis, A., Davies, A.G., and Linfield, E.H., ‘Terahertz quantum cascade lasers with >1 W output powers’, *Electron. Lett.*, 2014, **50**, pp. 309–311
- Hübbers, H.W., Pavlov, S., Semenov, A., Köhler, R., Mahler, L., Tredicucci, A., Beere, H., Ritchie, D., and Linfield, E., ‘Terahertz quantum cascade laser as local oscillator in a heterodyne receiver’, *Opt. Express*, 2005, **13**, pp. 5890–5896
- Tonouchi, M., ‘Cutting-edge terahertz technology’, *Nat. Photonics*, 2007, **1**, pp. 97–105
- Wanke, M.C., Young, E.W., Nordquist, C.D., Cich, M.J., Grine, A.D., Fuller, C.T., Reno, J.L., and Lee, M., ‘Monolithically integrated solid-state terahertz transceivers’, *Nat. Photonics*, 2010, **4**, pp. 565–569
- Adam, A.J.L., Kašalynas, I., Hovenier, J.N., Klaassen, T.O., Gao, J.R., Orlova, E.E., Williams, B.S., Kumar, S., Hu, Q., and Reno, J.L., ‘Beam patterns of terahertz quantum cascade lasers with subwavelength cavity dimensions’, *Appl. Phys. Lett.*, 2006, **88**, pp. 151105–151105–3
- Amanti, M.I., Fischer, M., Scalari, G., Beck, M., and Faist, J., ‘Low-divergence single-mode terahertz quantum cascade laser’, *Nat. Photonics*, 2009, **3**, pp. 586–590
- Yu, N., Wang, Q.J., Kats, M.A., Fan, J.A., Khanna, S.P., Li, L., Davies, A.G., Linfield, E.H., and Capasso, F., ‘Designer spoof surface plasmon structures collimate terahertz laser beams’, *Nat. Mater.*, 2010, **9**, pp. 73–75
- Amanti, M., Fischer, M., Walther, C., Scalari, G., and Faist, J., ‘Horn antennas for terahertz quantum cascade lasers’, *Electron. Lett.*, 2007, **43**, pp. 573–574
- Lee, A.W.M., Qin, Q., Kumar, S., Williams, B.S., Hu, Q., and Reno, J.L., ‘High-power and high-temperature THz quantum-cascade lasers based on lens-coupled metal-metal waveguides’, *Opt. Lett.*, 2007, **32**, pp. 2840–2842
- Scalari, G., Ajili, L., Faist, J., Beere, H., Linfield, E., Ritchie, D., and Davies, G., ‘Far-infrared ($\lambda \approx 87 \mu\text{m}$) bound-to-continuum quantum-cascade lasers operating up to 90 K’, *Appl. Phys. Lett.*, 2003, **82**, pp. 3165–3167
- Williams, B.S., Kumar, S., Callebaut, H., Hu, Q., and Reno, J.L., ‘Terahertz quantum-cascade laser at $\lambda \approx 100 \mu\text{m}$ using metal waveguide for mode confinement’, *Appl. Phys. Lett.*, 2003, **83**, pp. 2124–2126